

## Chitosan and Carboxymethylchitosan as High Turbidity Water Biocoagulants

Raimundo N. Lima Júnior<sup>1</sup>, João L. I. O. Almeida<sup>1</sup>, Jones de Andrade<sup>2</sup> and Flávia O. M. S. Abreu<sup>1,\*</sup>

<sup>1</sup>Natural Sciences Program, State University of Ceará-UECE, Fortaleza, CE 60714-903, Brazil

<sup>2</sup>Physical-Chemistry Department, Institute of Chemistry, Federal University of Rio Grande do Sul-UFRGS, Porto Alegre, RS 91501-970, Brazil

\*Corresponding Author: Flávia O. M. S. Abreu. Email: flavia.monteiro@uece.br

Received: 20 May 2020; Accepted: 09 July 2020

**Abstract:** Biocoagulants emerges as a promising technology in water treatment, in order to exploit renewable and biodegradable materials. The present work aims to study the coagulant action of chitosan and carboxymethylchitosan on water with very high turbidity (above 300 NTU), contrasting the physicochemical results with those obtained for aluminum sulphate. Carboxymethylchitosan was produced by the Williamson's ethers synthesis and characterized by potentiometric titration, FTIR and <sup>1</sup>H-NMR. The coagulant tests were performed using synthetic water in a Jar-test equipment, through the induction of high and low velocity gradients, followed by sedimentation. The results showed turbidity and color removal efficiencies above 99% for the biocoagulants, by applying dosages much lower than those used for aluminum sulphate; the volume of sedimentable solids obtained at the end of the water treatment process was much lower when chitosan and carboxymethylchitosan were used as coagulants (reduction of 25% when compared to aluminum sulphate). In summary, carboxymethylchitosan is a non-toxic, renewable, biodegradable material with high efficiency as a coagulant for waters with very high turbidity, showing promise for in natura applications.

**Keywords:** Chitosan; carboxymethylchitosan; biocoagulants; colloids and interfaces

### 1 Introduction

One of the main physicochemical parameters evaluated in the natural water treatment and quality is turbidity, which is characterized by the presence of suspended materials (clay, silt, sludge, organic matter and excess of microorganisms) that cause absorption and/or dispersion of light. This parameter can be dramatically increased as a result of natural phenomena, such as floods, storms and typhoons, or as a consequence of anthropogenic activities, such as domestic and industrial sewage releases and spillage of mining tailings in water bodies [1]. Water turbidity can be classified as low (less than 50 NTU), medium (50–100 NTU), high (100–200 NTU) and very high (above 300 NTU). In natural water, high turbidity levels may interfere with the photosynthetic reactions, which are essential for ecosystem balance. The efficiency and safety of water treatment processes for public water supply depend on the lower levels of residual turbidity, especially from the microbiological point of view [2,3].



This work is licensed under a Creative Commons Attribution 4.0 International License, which permits unrestricted use, distribution, and reproduction in any medium, provided the original work is properly cited.

Inorganic salts, such as aluminum sulphate, ferric chloride, ferrous sulfate and aluminum polychloride are routinely used as coagulants for water treatment. A current concern is the residual of these elements in treated water, especially aluminum. Several studies point out the danger of human exposure to this metal, correlating it with neurodegenerative diseases such as Alzheimer's disease [4,5].

Chitosan (CT) is a linear copolymer formed by units of D-glucosamine and *N*-acetyl-D-glucosamine, obtained by the deacetylation reaction in an alkaline medium of chitin, one of the most abundant polysaccharides on the planet. The increasing interest in the use of CT as a coagulant for the treatment of water supply and waste water is based on the various operational and environmental advantages that can be obtained, such as high efficiency in removal of suspended solids and metal ions, low required dosage when compared to inorganic coagulants, formation of dense flakes and biodegradable sludge production [6–8].

As a disadvantage, chitosan exhibits a solubility limited to acidic media, typically at pH less than 6.5. The structural modifications of the polymer appear as a methodology for optimizing the properties of the derived materials. Carboxymethylchitosan (CMC) is one of the most studied ones nowadays, which is obtained by the insertion of carboxymethyl groups (-CH<sub>2</sub>-COOH), replacing the hydrogens present in the amino (-NH<sub>2</sub>) and hydroxyl groups (-OH), which are abundant in the chitosan structure. CMC has the advantages of solubility in a wide range of pH, low toxicity, biodegradability, ability of gel formation and inhibition on the development of bacterial biofilms [9,10].

In view of the promising perspectives of the use of chitosan for the natural water treatment, this work aims to study the coagulant action of this biopolymer on very high turbidity synthetic water, quantitatively evaluating the efficiency in the removal of apparent color, turbidity, sedimentable solids formation and its influence on the electrical conductivity, alkalinity and pH of the medium. In parallel, we make a comparative of operational efficiency among chitosan, aluminum sulfate and the carboxymethylchitosan synthesized from the chitosan reaction with monochloroacetic acid in a strongly alkaline medium.

## 2 Materials and Method

### 2.1 Synthesis of Carboxymethylchitosan

Carboxymethylchitosan (CMC) was obtained according to a methodology described by Abreu et al. [11] through the Williamson's ethers synthesis reaction, where 1 g of CT (Polymar-Brasil, Degree of deacetylation = 71.8%,  $M_w = 3.3 \times 10^5 \text{ g mol}^{-1}$ ), suspended in 21.5 mL of isopropanol, reacted with monochloroacetic acid (C<sub>2</sub>H<sub>3</sub>O<sub>2</sub>Cl), 3 g or 6 g, alkaline medium (NaOH), 3 mol L<sup>-1</sup> or 6 mol L<sup>-1</sup>, for 4 h at 50°C under constant stirring. The resulting product was successively washed with ethanol (80% and 90%) and methanol (analytical grade, Dinamica) and dried in the oven at 60°C for 24 h. Four experiments were performed in duplicate for each dependent variable, grouped into blocks of 2 randomly selected experiments to minimize nuisance effects. The planning matrix containing the independent

**Table 1:** Reaction conditions of CMC synthesis and degree of substitution of CMC samples

Sample	C <sub>NaOH</sub> (mol L <sup>-1</sup> ) <sup>b</sup>	Acid: CT <sup>a</sup>	DS (%)	
			FTIR	Titration
CMC38	3	3:1	43.2	32.7 ± 2.1
CMC42	6	3:1	45.7	38.9 ± 1.7
CMC44	3	6:1	47.0	41.2 ± 2.3
CMC59	6	6:1	61.4	56.2 ± 2.5

<sup>a</sup>Mass ratio between acid and polymer.

<sup>b</sup>Base concentration.

variables and the corresponding substitution degree are in [Tab. 1](#). The statistical treatment of the data was performed through ANOVA analysis in the Excel program (Microsoft 2010), using confidence level of 95%.

## 2.2 Characterization of Chitosan and Carboxymethylchitosan

### 2.2.1 Potentiometric Titration

The potentiometric titration, with pH meter Luca-210, was used to calculate the degrees of deacetylation (DD) and substitution (DS) of chitosan and carboxymethylchitosan synthesized respectively, described in the literature [[11](#),[12](#)]. Titrations were carried out in duplicate, based on the reaction between KOH and each biopolymer, previously dissolved in HCl, according to [Eqs. \(1\) and \(2\)](#):

$$DD_{Chitosan} (\%) = \left( \frac{M_{KOH} \times (V_2 - V_1) \times 161}{mCT} \right) \times 100 \quad (1)$$

$$DS_{CMQ} (\%) = \frac{161 \times (M_{KOH} \times V_{KOH})}{mCMC - 58 \times (M_{KOH} \times V_{KOH})} \quad (2)$$

where:  $M_{KOH}$  and  $V_{KOH}$  are the molarity and the volume of titrant base solution (KOH),  $(V_2 - V_1)$  is the volume in liters of the base solution consumed between the first and second titration equivalence points,  $mCT$  and  $mCMC$  are the masses of chitosan and carboxymethylchitosan (g) used, and 161 and 58 are the molar masses of the chitosan repeating units (D-glucosamine) and the titrated carboxymethyl groups ( $-CH_2-COO^-$ ), respectively.

### 2.3 Fourier Transform Infrared Spectroscopy (FT-IR) and Zeta Potential

Infrared spectroscopy was used to evaluate the degree of deacetylation of chitosan and the degree of substitution in the carboxymethylation reaction through the analysis of characteristic bands. Measurements were made on a Nicolet iS5 spectrometer from Thermo Scientific, and the samples were prepared as KBr pellets in the ratio of 1:20 (m/m). Chitosan DD and carboxymethylchitosan DS were calculated based on [Eqs. \(3\) and \(4\)](#) proposed in the methodologies of Brugnerotto et al. [[13](#)] and Borsagli et al. [[10](#)] which interrelate the band absorbance of *N*-acetyl-D-glucosamine (A1,320), D-glucosamine (A1,420) and amino groups (A1,624) with carboxymethyl groups (A1,745).

$$DD (\%)_{Chitosan} = 100 - \left[ 31.92 \times \left( \frac{A_{1,320}}{A_{1,420}} \right) - 12.20 \right] \quad (3)$$

$$DS (\%)_{CMQ} = \left\{ 1 - \left[ \left( \frac{A_{1,624}}{A_{1,745}} \right) / 1.33 \right] \right\} \times 100\% \quad (4)$$

Zeta potential were determined by dynamic light scattering using the Malvern Zetasizer equipment (Malvern Instruments, United Kingdom). Approximately 10 mg of the samples were dispersed 50 ml of buffered solution at pH 3, pH 7 and pH 9, and left in agitation for 12 h prior to measurements. The values were acquired in triplicate.

#### 2.3.1 Proton Nuclear Magnetic Resonance Spectroscopy ( $^1H$ -NMR)

$^1H$ -NMR was employed to further verify the carboxymethylation of the chitosan. Each one of the carboxymethylchitosan samples (~10 mg) were dissolved in 1 mL of  $D_2O$  provided by Aldrich Chemical Company. Half an hour later, each one of the samples was vacuum filtered through a cotton filter with brand-new Pasteur pipettes to separate the solution from the still undissolved carboxymethylchitosan. The samples were then analyzed in a Bruker Ascend 400 MHz NMR spectrometer at 25°C in NMR network

of UFRGS. DHO signal position was adjusted for each temperature accordingly to expressions provided by Gottlieb et al. [14]. Carboxymethylchitosan deacetylation degree (DD) was successfully evaluated with Eq. 5, from Borsagli et al. [10]. The degree of substitution (DS) was calculated for each substitution site independently with Eqs. (6)–(8), and combined in Eqs. (9) and (10), provided by Chen et al. [15] and Ragnhild et al. [16].

$$DD.^{NMR}(\text{Chitosan}) = 100 - \left[ \frac{A_{CH_3}/3}{A_{C_2}} \right] \cdot 100\% \quad (5)$$

$$DS.^{NMR}(C3) = \frac{A_{C_3^{cm}}}{A_{C_1^{ac}} + A_{C_2^{des}}} \cdot 100\% \quad (6)$$

$$DS.^{NMR}(C6) = \frac{1}{2} \frac{A_{C_3^{cm}} + A_{C_6^{cm}} - A_{C_3^{cm}}}{A_{C_1^{ac}} + A_{C_2^{des}}} \cdot 100\% \quad (7)$$

$$DS.^{NMR}(N) = \frac{1}{2} \frac{A_{N^{cm}}}{A_{C_1^{ac}} + A_{C_2^{des}}} \cdot 100\% \quad (8)$$

$$DS.^{NMR}(O) = DS.^{NMR}(C3) + DS.^{NMR}(C6) \quad (9)$$

$$DS.^{NMR}(CMQ) = DS.^{NMR}(O) + DS.^{NMR}(N) \quad (10)$$

were  $C_2^{des}$  is corresponding to intensity of peak from the hydrogen atom of desacetylated glucosamine,  $C_{3-6}$  and  $C_2^{ac}$  from atoms from C3 and C6 and from acetylated glucosamine  $C_2$ ,  $C_6^{cm}$  and  $C_3^{cm}$  is from hydrogen in carboxymethyl groups in  $C_6$  an  $C_3$ ,  $N^{cm}$  is from the protons of amino groups in  $C_2$  and  $C_1^{des}$  is from acetylated glucosamine rings.

### 2.3.2 Preparation of Synthetic Water and Coagulant Solutions

Samples of synthetic water with turbidity between 1,500 and 1,650 NTU and apparent color between 500 and 800 uC were prepared in two batches. Silt-rich sediment was dispersed in distilled water (5% w/v), and then vigorously stirred for 20 min and finally settled for 6 h. Afterwards, the supernatant was siphoned into another vessel and stored for coagulation tests. Fine adjustments were made for the desired color and turbidity by dissolving extra small amounts of silt or by adding distilled water to the siphoned fraction. Tab. 2 provides physicochemical parameters of synthetic water before treatment.

**Table 2:** Physico-chemical parameters of synthetic water before treatment

Parameter	Methodology	Value
pH	Potentiometry	6.42–7.45
Apparent Color (uC)	Colorimetric comparison	500–800
Turbidity (NTU)	Turbidimetry	1500–1650
Electric conductivity at 25°C (μS/cm)	Conduitimetry	30.80–54.27
Alkalinity (mg l <sup>-1</sup> CaCO <sub>3</sub> )	Acid-base titration	30–45

Coagulant solutions of chitosan and carboxymethylchitosan were prepared by previously dissolving 500 mg of each compound in 50 mL of 0.1 M HCl and shaking for 18 h. After this period, each mixture was transferred to a 100 mL volumetric flask and calibrated with 0.1 M HCl, giving a 5,000 mg L<sup>-1</sup>

stock solution. Aqueous solutions of aluminum sulfate were prepared in the same concentration as above, starting from the analytical grade solid reagent.

### 2.3.3 Coagulation Assays—Jar Test and Other Parameters

The coagulation/flocculation assays were performed in Milan *Jar-Test* equipment, JT 102 model, provided with 03 acrylic vats. In each assay, the evaluated coagulant was added to 1 L of synthetic water, which was subjected to rapid mixing at 200 rpm for 2 min, and then slow mixing at 40 rpm for 20 min. Soon after, the system was switched off and allowed to settle for 20 min. Supernatant samples (2 cm below the surface) were carefully removed for physicochemical evaluation and measurement of the efficiency of each process. When necessary, solutions of HCl and 0.1 M NaOH were used to adjust the pH of the medium. Turbidity (NTU), Apparent Color (uC), pH, Electrical Conductivity at 25°C ( $\mu\text{S}/\text{cm}$ ), Alkalinity ( $\text{mg l}^{-1} \text{CaCO}_3$ ) and Sedimetric Solids ( $\text{mL l}^{-1}$ ) parameters were used to analyze the influence of each coagulant under study on the physicochemical characteristics of the treated water, as described in Standard Methods [17]. The turbidity and color removal efficiencies were estimated in percentage terms, according to Eqs. (11) and (12), respectively.

$$\% \text{Removal}_{\text{Turbidity}}(T) = \left( \frac{T_{\text{initial}} - T_{\text{last}}}{T_{\text{initial}}} \right) \times 100 \quad (11)$$

$$\% \text{Removal}_{\text{Color}}(C) = \left( \frac{C_{\text{initial}} - C_{\text{last}}}{C_{\text{initial}}} \right) \times 100 \quad (12)$$

## 3 Results and Discussions

### 3.1 Properties of Chitosan and Carboxymethylchitosan

Fig. 1. shows the infrared spectra of chitosan and carboxymethylchitosans. The major changes studied were observed in the range of 1,000–2,000  $\text{cm}^{-1}$ . It is possible to observe the presence of chitosan typical bands, located at 1633 and 1557  $\text{cm}^{-1}$ , corresponding to the symmetric and asymmetric stretching, respectively, of amide I and II. The insertion of the carboxymethyl groups in the chitosan, especially in the acid form, is evidenced by the appearance of a new absorption band at 1,745  $\text{cm}^{-1}$ , associated with the formation of carboxylic dimers through intermolecular interactions. It is also seen that the 1,654  $\text{cm}^{-1}$  amide I band, initially present on chitosan, shifted to 1,624  $\text{cm}^{-1}$ , due to the hydrogen bonds established

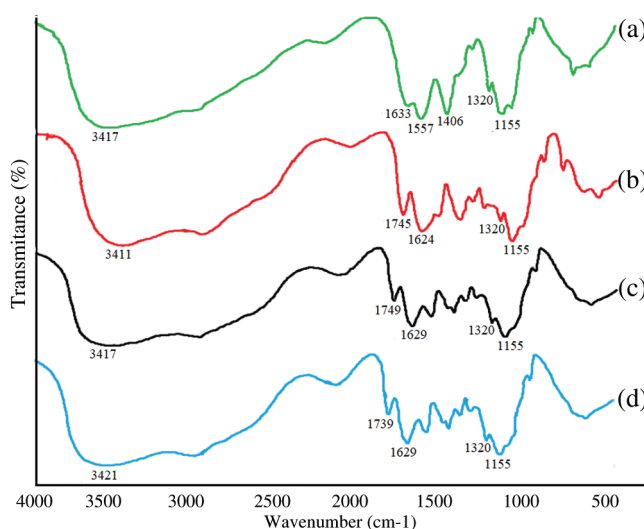


**Figure 1:** Infrared Spectra of CT (a), CMC59 (b), CMC44 (c), CMC38 (d)

between the amide and carboxyl groups. The reduction in the intensity of the bands at  $1,155\text{ cm}^{-1}$  (C-O-C) and  $1,320\text{ cm}^{-1}$  (amide III) may be associated with the conformational and structural modifications resulting from the hydroxylic hydrogen's substitutions of the chitosan carbons 6 and 3 by carboxymethyl groups [11,18].

The degree of deacetylation (DD) of the chitosan obtained by FTIR and by titration were, respectively, 72.9 and  $71.8 \pm 1.1\%$ , and there was an excellent correlation between the different methods. The degree of substitution (DS) was obtained for Carboxymethylchitosan by titration and FTIR techniques are presented in Tab. 1.

ANOVA analysis showed that both NaOH concentration (factor A) and chloroacetic acid:CT mass ratio (B), were significant factors on the substitution degree, verified by the significance analysis, where  $F_0$  was greater than F significance as can be seen in Tab. 3.

**Table 3:** ANOVA Analysis Results

Parameters	Sum Square	Degree of freedom	Median square	Fo	Fo Tab	
A	181.45	1	181.45	<b>6.684</b>	6.03	Significant
B	256.51	1	256.51	<b>9.449</b>	6.03	Significant
AB	53.56	1	53.56	<b>1.973</b>	6.03	Not significant
Error	108.59	4	27.15			
Total	600.1					

A-NaOH concentration (mol/L); Low level (-1): 3 mol/L; High level (+1) 7 mol/L; B-Chloroacetic Acid/Chitosan mass ratio Low level (-1): 3:1; High level (+1) 6:1

This result is in accordance with the literature. Chen et al. [15] discussed that with the increase in the alkaline concentration, the -OH groups of carbons 3 and 6 from chitosan can act as a strong nucleophile and react with the chloroacetic acid via Williamson mechanism, which can lead to a higher DS. On the other hand, in the results obtained by Abreu et al. [19], when chloroacetic acid is used in higher content, a greater degree of substitution can be achieved. In this case, the addition of chloroacetic acid in excess is needed due to the tendency to form side reactions over time with  $\text{OH}^-$ , reducing its concentration in reactional medium. In our study, using both parameters CT:Ac ratio and NaOH in higher level it was obtained an average increase of 28% on the DS, evident from FTIR and Titration determination methods.

### 3.2 $^1\text{H-NMR}$ Spectrogram

The  $^1\text{H-NMR}$  spectrograms measured at  $25^\circ\text{C}$  for the carboxymethylchitosan samples are displayed at Fig. 2. The signal at  $\delta = 2.01$  ppm is assigned to the methylic hydrogen atoms (3 protons) from acetamide ( $-\text{NH}-\text{CO}-\text{CH}_3$ ) groups from the original chitosan structure. From glucosamine rings there is the broader signal at  $\delta = 3.12$  ppm from the hydrogen atom of desacetylated glucosamine C2 (1 proton,  $\text{C}_2^{\text{des}}$ ). Also, from glucosamine rings there are the two broad signals starting at  $\delta = 3.60$  ppm and ending around  $\delta = 4.02$  ppm, both originated from the resonance of hydrogen atoms from C3 to C6 and from acetylated glucosamine C2 (6 protons,  $\text{C}_{3-6} + \text{C}_2^{\text{ac}}$ ). Concerning the carboxymethyl groups, their presence is firstly indicated by the  $\delta = 4.09$  ppm sharp signal, related to C3 and C6 (2 and 1 protons respectively,  $\text{C}_6^{\text{cm}} + \text{C}_3^{\text{cm}}$ ) hydroxyl groups being consumed in the O-carboxymethylation reaction ( $-\text{O}-\text{CH}_2-\text{COO}^-$ ). The sharp signal observed at  $\delta = 4.28$  ppm is another indication of O-carboxymethylation reaction, this turn only at the C3 (1 proton,  $\text{C}_3^{\text{cm}}$ ) hydroxyl group location. The spectrogram measured also provides only very small signals at  $\delta = 3.25$  ppm, suggesting a very low degree of N-carboxymethylation (formation of  $-\text{N}-\text{CH}_2-\text{COO}^-$ ) at the amino groups (2 protons,  $\text{N}^{\text{cm}}$ ) under the reaction conditions investigated. The C1 hydrogen atom signal from acetylated glucosamine rings (1 proton,  $\text{C}_1^{\text{ac}}$ ) appears at

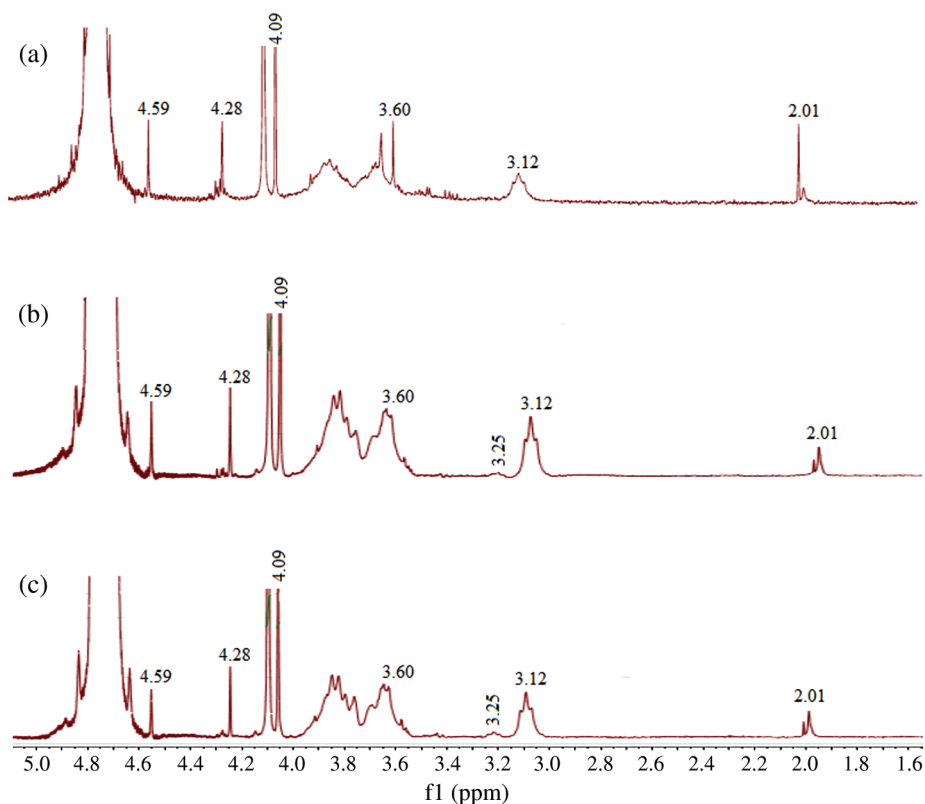


**Figure 2:**  $^1\text{H-NMR}$  Spectrogram of CMC59 (a), CMC44 (b), CMC38 (c)

4.59 ppm. On the other hand, the C1 hydrogen atom signal for the deacetylated glucosamine rings (1 proton,  $\text{C}_1^{\text{des}}$ ) appears around 4.81 ppm and was superposed by the DHO signal at 25°C. These signals assignments agree with previously published spectrograms [10,15,16].

For the samples CMC44 and CMC38 it can be observed signals at  $\delta = 3.25$  ppm, suggesting a low degree of N-carboxymethylation (formation of  $-\text{N}-\text{CH}_2-\text{COO}^-$ ) at the amino groups under the reaction conditions investigated. These samples were produced with lower hydroxyl concentration. In another study, Chen et al. [15] showed that the alkaline medium influenced on the N-carboxymethylation degree,

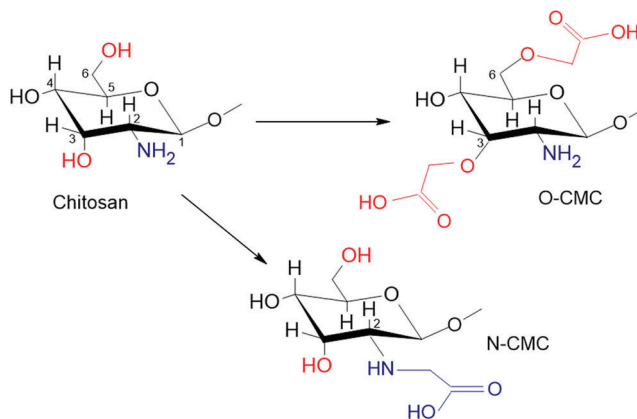


**Figure 3:** Carboxymethylchitosan structure formation from chitosan. Hydroxyl sites (positions 3 and 6, red color) and amino site (position 2, blue color)

where with lower hydroxyls concentration can lead to some degree of substitution on the amino sites (-NH<sub>2</sub>). Fig. 3 shows the Carboxymethylchitosan structure highlighting the hydroxyl and amino sites.

The degree of deacetylation (DD) of the chitosan and the degree of substitution (DS) of the carboxymethylchitosan (both total and for each individual site) are provided in Tab. 4. The degree of deacetylation (DD) of the chitosan obtained by <sup>1</sup>H-NMR was between 88.90% and 93.17% from all samples. The degree of substitution (DS) of the carboxymethylchitosan samples presented mean values ranging between 40.17% and 46.70%. The calculated DS is a quantitative measurement on the total content of hydrogens replaced by -CH<sub>2</sub>-COOH groups, measure from the amount of either hydroxyl (O-CMC) sites and amino (N-CMC) sites. The specific substitution at hydroxyl groups from glucosamine atoms C3 and C6 and from amine groups at C2, presented values between 12.4% and 27.1%, 14.3% and 33.0% and 1.26% and 3.63%, respectively. It is evidenced that the carboxymethylation reaction, under the investigated reaction conditions, strongly favors the hydroxyl sites over the amino groups.

**Table 4:** DS percentuals determined by <sup>1</sup>H-NMR, as well as DS(C3), DS(C6), DS(N) and DS(O) individually determined by <sup>1</sup>H-NMR from peak integration

	<sup>1</sup> H-NMR					
	DD	DS(3)	DS(6)	DS(N)	DS(O)	DS
CMC38	92.79	17.56	18.99	3.63	36.55	40.17
CMC44	92.61	12.43	33.01	1.26	45.44	46.70
CMC59	89.04	27.10	14.28	1.71	41.39	43.11

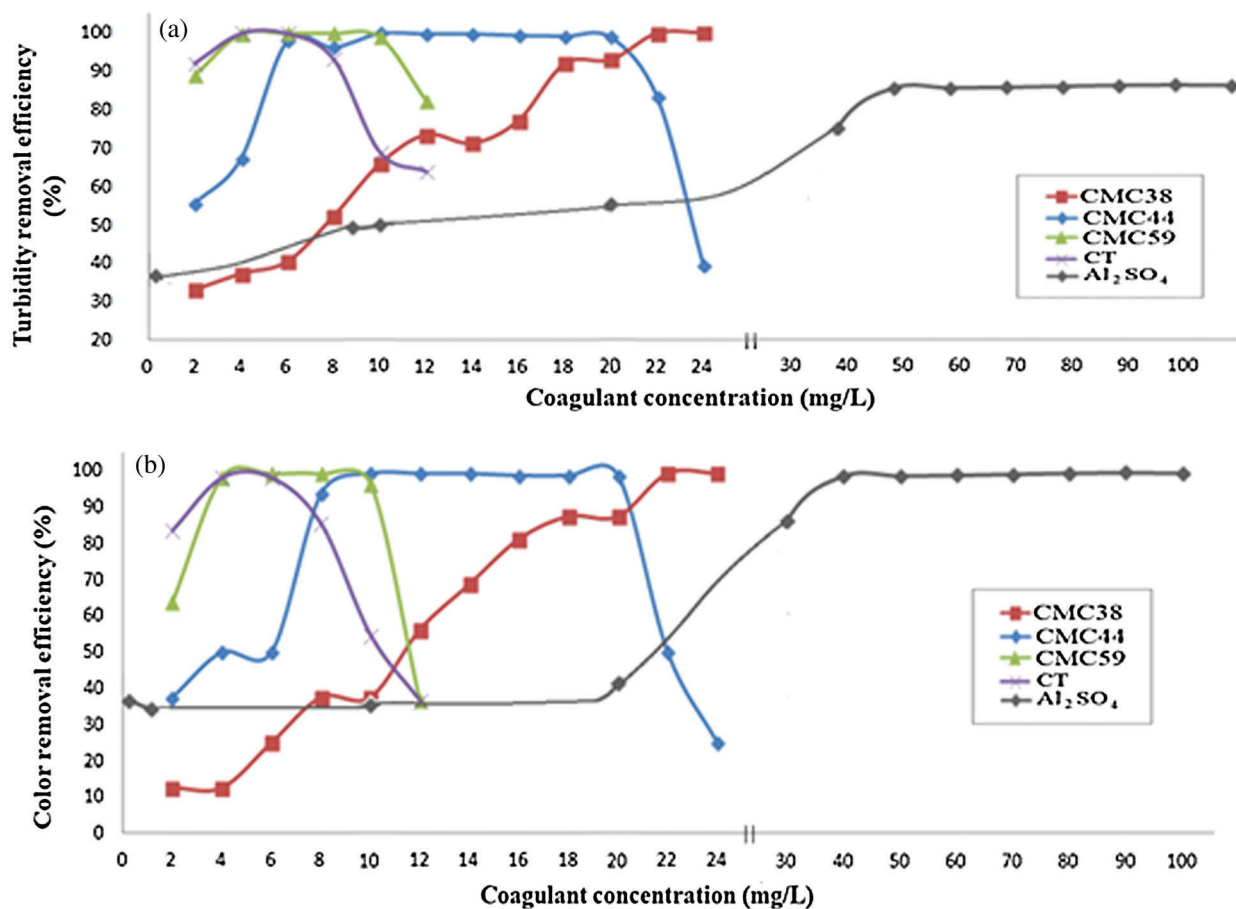
The carboxymethylation reaction, when conducted in a strongly alkaline medium, favors the activation of the hydroxyls present in the chitosan, which can lead to the majority formation of O-CMC, maintaining the amino sites (-NH<sub>2</sub>) [10]. In this study, a low DS on N-CMC sites is fundamental for the coagulant activity of the material.

### 3.3 Study of Color and Turbidity Removal Efficiency

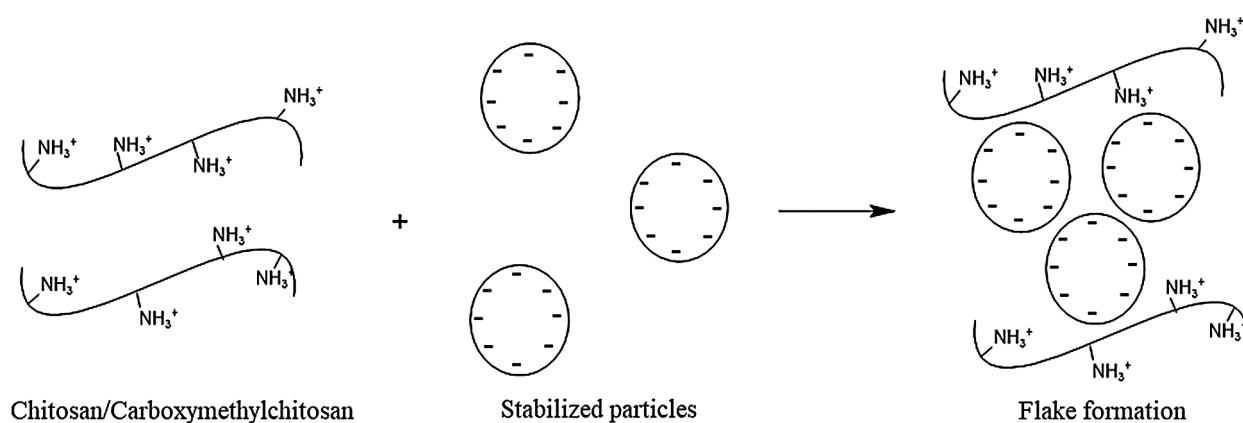
Fig. 4 shows the comparative results obtained in the coagulation tests using chitosan (CT), CMC44, CMC38 and CMC59 and aluminium sulfate as turbidity and apparent color removal agents. The higher efficiency of biocoagulants is associated with the chemical structure and mechanisms of action of each one of them.

Fig. 5 shows the schematic representation of the flocculation process. The initial dissolution in acid medium allows the protonation of the amino groups present along the chitosan and carboxymethylchitosan chains. The cationic polyelectrolytes are capable of neutralizing/reducing the surface charges of suspended particles (which usually present negative surface charge), allowing their aggregation, and the formation of dense flakes, which sediment rapidly. The formation of intrachain bridges also allows the creation of an adsorbent network that collaborates to remove the particulate present in the medium [6,20]. When the formation of the *N*-carboxymethylated product occurs, there is a reduction in the amino groups of the polysaccharide chain, which influences in the efficiency of the sample.

The biocoagulants showed the best results, with optimum dosages of 4 to 5 mg l<sup>-1</sup> for chitosan and 6 to 7 mg l<sup>-1</sup> for CMC59. For Al<sub>2</sub>(SO<sub>4</sub>)<sub>3</sub>, equivalent yields were only obtained using dosages of 90 mg l<sup>-1</sup>. Fig. 4 show that chitosan and carboxymethylchitosan exhibit maximum results of operational efficiency for each coagulant, consuming amounts 12 to 18 times lower than those required for aluminum sulphate, combining high efficiency and low material consumption. Sánchez-Martín et al. [21] had already reported the low operational efficiency of aluminum sulphate (applied in dosages of 15 mg l<sup>-1</sup>) when compared to several other biocoagulants, such as those based on the seeds of the *Moringa oleifera* (Lam) species and vegetable tannins.



**Figure 4:** Turbidity Removal Efficiency (a) and Apparent Color removal efficiency (b) for chitosan (CT), carboxymethylchitosan samples (CMC) and Aluminum Sulfate as Coagulants



**Figure 5:** Schematic representation of the Flocculation process

The decrease in the chitosan coagulant efficiency, observed from concentrations of  $8.0 \text{ mg l}^{-1}$ , is associated with the excess of positive charges added to the medium ( $-\text{NH}_3^+$ ), which contribute to the re-stabilization of the suspended material. For CMC59, a wide range of concentrations with high coagulant

efficiency indexes ( $3\text{--}10\text{ mg l}^{-1}$ ) is observed; the re-stabilization, resulting from the reversal of surface loads of the suspended material, only starts from  $11\text{ mg l}^{-1}$  dosages, being possible to use larger/smaller dosages without significant efficiency losses.

The results obtained for chitosan and carboxymethylchitosan are promising, especially when considering prospects of practical application, health safety and operational efficiency in comparison with other natural coagulants derived of CT described in the literature. Yang et al. [22], reported the use of amphoteric chitosan-based flocculant (3-chloro-2-hydroxypropyl trimethyl ammonium chloride modified carboxymethyl chitosan) in the removal of turbidity from synthetic waters, obtaining removals of 88.4% before sand filtration and 98.9% after sand filtration. Zhao et al. [23], studied O-Phosphorylate Chitosan in the removal of turbidity obtaining 90% of efficiency with an optimum dosage of  $20\text{ mg l}^{-1}$ . Oladoja et al. [24], perform coagulant studies with the aqueous extracts of the seeds of *Margaritarea discoidea* (Baill.) G.L. Webster on synthetic raw waters, obtaining removals of turbidity above 90% in all evaluated dosages. However, a drawback observed in the research was the appearance of greenish coloration in the treated water, proportional to the increase of the biocoagulant concentration in the medium. Abidin et al. [25], studied the coagulant efficiency of the extract of the seeds of the *Jatropha curcas* L. (jatropha) on synthetic wastewater, obtaining yields of 99.4% of removal of turbidity with the use of  $120\text{ mg l}^{-1}$ . However, this last biocoagulant has the disadvantage of presenting toxic compounds in its seeds (phorbol esters and allergenic proteins) that require a previous treatment of the material. The operational efficiencies of chitosan and carboxymethylchitosan are similar to those observed for vegetable tannin-based biocoagulants available in the market (Tanfloc and Silvafloc), which, although efficient (removal of particulate matter above 99%), require several production steps (via Mannich Reaction) until the final product is obtained.

The operational performance of the two biocoagulants evaluated for removal of color and turbidity corroborate previous works, such as the one conducted by Altaher [2], which developed studies on the use of chitosan as a biocoagulant in the preconditioning of seawater used for reverse osmosis, aiming at the removal of excess solids in suspension leached by the rains. The results showed efficiencies of the removal of turbidity higher than 97%, using  $18\text{ mg l}^{-1}$  dosages of the biopolymer, strongly contrasting with the high concentrations of aluminum sulphate ( $1,200\text{ mg l}^{-1}$ ) required to achieve equivalent operational results. In summary, CT and CMC from our study presented 99% of turbidity and color efficiency removal without any further purification process, using dosages considerable lower than other coagulants and biocoagulants from literature, which states the potentially for the use as effective lowcost biocoagulant.

### **3.4 Influence of the Coagulants Evaluated on the pH and Alkalinity of the Treated Water**

The low efficiency observed for  $\text{Al}_2(\text{SO}_4)_3$ , reflected in optimal dosages well above those obtained for the evaluated biocoagulants, may be related to its chemical behavior in the solution. Aluminum sulphate behaves as a strong acid when dissolved in water (a direct consequence of successive hydrolysis reactions that generate  $\text{H}_3\text{O}^+$  cations), decreasing the pH and consuming the alkalinity of the medium. These changes directly affect the coagulation phenomenon, which for  $\text{Al}_2(\text{SO}_4)_3$  ideally occurs in the range of pH 5.5–6.5 [26]. Khodapanah et al. [27], in a comparative study between the efficiencies of different biocoagulants and aluminum sulphate, demonstrated that after the treatment there was a reduction of the water pH from 6.4 to 5.1, with the application of  $20\text{ mg l}^{-1}$  dosages to obtain satisfactory yields.

Analogous behavior regarding the pH was observed for chitosan and CMC59, mainly due to the use of HCl in the preparation of the coagulant solution. However, the dosages required to achieve optimum conditions of removal of apparent color and turbidity implied in small variations in the final pH of the treated water (2.96% for chitosan using  $4.0\text{ mg l}^{-1}$  and 13.08% for CMC using  $7.0\text{ mg l}^{-1}$ ). The maintenance of the water pH (or low variation in the case of the present study) is a characteristic

presented by most of the currently studied biocoagulants, such as those derived from vegetable tannins, angiosperm seeds (*Moringa oleifera* and *Jatropha curcas*) and cactaceae (*Opuntia* spp.). However, Oladoja et al. [24], demonstrated that the aqueous extract of the seeds of the *Margaritarea discoidea* species, when applied as a biocoagulant, is able to naturally reduce the final pH of the treated water.

The analysis of the total alkalinity variation of the water treated with chitosan and CMC59 revealed significant differences between the two biocoagulants. For chitosan, no variation in this parameter was observed, probably due to the mechanisms involved in the removal of suspended particulate matter, which do not include the alkalinity consumption of the medium, but rather the neutralization of loads and the formation of adsorbent intrachain bridges of impurities [20]. As a consequence, we discard a possible interference of the HCl used in the preparation of the coagulant solutions on the total alkalinity results, which is characterized by the presence of basic anions in the water (carbonates, bicarbonates and hydroxides) [8].

For the carboxymethylchitosan, a progressive consumption of water alkalinity was observed, probably due to the presence of the new carboxymethyl groups, which react preferentially with the  $\text{HCO}_3^-$  ions of the medium (present mainly in the pH range of the synthetic raw water) through acid-base reactions. This characteristic is uncommon among biocoagulants (which mostly do not consume the alkalinity of the medium) and may pave the way for the production of new materials applicable to waste treatment systems with high turbidity, color and alkalinity, such as effluents of the pulp and paper industry [28].

The consumption of water alkalinity during the biocoagulant treatment process was also reported by Edogbanya et al. [29], who developed bench studies using the seeds of the *Adansonia digitata* L species (a typical plant of the African continent) for this purpose. The results showed that ideal dosages for significant removals of turbidity and *Escherichia coli* ( $150\text{--}200\text{ mg l}^{-1}$ ) reduced the water alkalinity from 9.00 to 4.33  $\text{mg l}^{-1}$ .

### 3.5 Study of the Ideal Chitosan and Carboxymethylchitosan Coagulation pH

The study of the ideal coagulation of pH for CMC59 (achieved after acid/base additions subsequent to the coagulant application) is provided in Fig. 6.

Results showed that CMC59 had higher efficiencies for the removal of turbidity (Fig. 6a) and apparent color (Fig. 6b) in a broad pH range when compared to chitosan. Although it was used in higher concentrations, the carboxymethylchitosan allowed to obtain a residual turbidity of the supernatant of 0.39 NTU and apparent color in the magnitude of 5uC (without application of filtration in the decant mixture), corresponding to removal efficiencies of 99.97% and 99.00%, respectively, when the coagulation pH was maintained in the range of 4.0–4.5.

In a study carried out in Malaysia et al. [27] showed that chitosan showed high coagulant efficiency for the removal of turbidity from natural raw waters at pHs 4 and 5 (using  $0.5\text{ mg l}^{-1}$ ) and reduced activity in alkaline medium (pH 9), this way corroborating the findings of the present work. Altaher [2] also reported obtaining a residual turbidity of 0.43 NTU for chitosan-treated seawater (no need for pH corrections), with the subsequent application of filtration of the mixture decanted into sand bed.

The decrease in the chitosan coagulant efficiency, observed at pH above 8.0, may be associated to the precipitation of the biopolymer chains. Fig. 7 shows the variation of zeta potential as a function of pH. As the pH increases from 7 to 9, the chitosan  $-\text{NH}_3^+$  groups are gradually deprotonated, reaching the isoelectric point, where the insufficiency of electric charges causes instability and precipitation, in accordance with results from Liu et al. [30].

In an acidic medium, the solubility is due to the repulsion exerted between the protonated amino groups ( $-\text{NH}_3^+$ ), favoring greater interactions between polymer and solvent ( $\text{CT-NH}_3^+ - \text{H}_2\text{O} - ^+\text{H}_3\text{N-CT}$ ), which surpass the hydrophobic forces and associative hydrogen interactions between polymer chains [10].

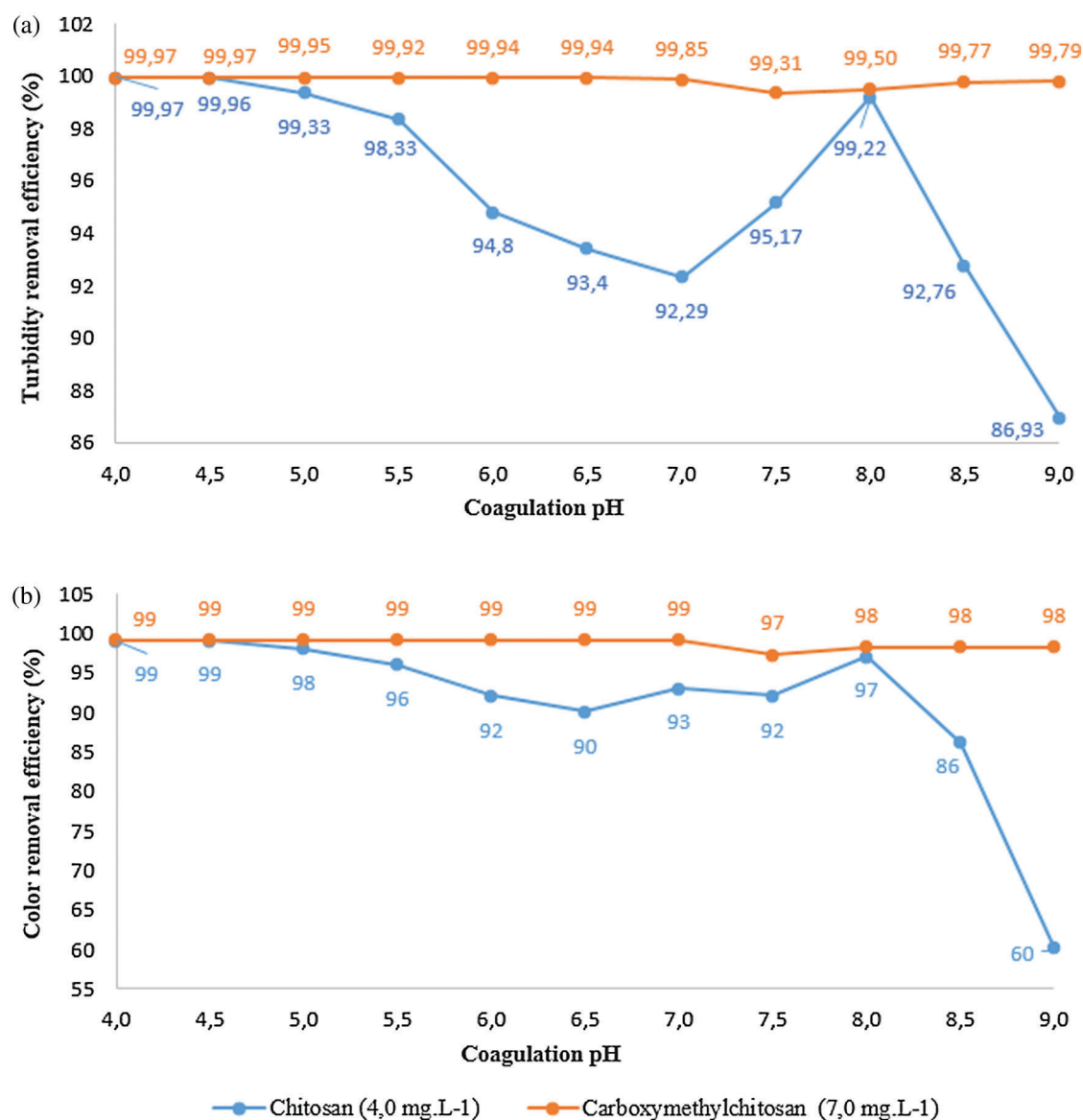


**Figure 6:** Influence of coagulation pH on the efficiency of chitosan and CMC59 in the removal of water turbidity (a) and apparent color (b)

For the carboxymethylchitosan, minimal variation in the coagulating effect is observed along the analyzed pH range (0.66% and 2.02% drop in turbidity and apparent color, respectively), possibly related to the amphotericism exhibited by amino ( $-\text{NH}_2$ ) and carboxymethyl ( $-\text{CH}_2\text{COOH}$ ) groups, which are mostly protonated in acid medium and deprotonated in basic medium (the carboxymethyl group deprotonates first during the pH increase). The formation of the carboxymethylated anions ( $-\text{CH}_2\text{COO}^-$ ) in alkaline medium contributes to the expansion of the carboxymethylchitosan solubility range and preservation of the coagulant effect by promoting repulsion between the negative charge chains ( $\text{CMC}^- - \text{CMC}^- - \text{CMC}^-$ ) and higher intermolecular interactions between polymer and water ( $\text{CMC}^- - \text{HOH}^- - \text{CMC}^-$ ) [31].

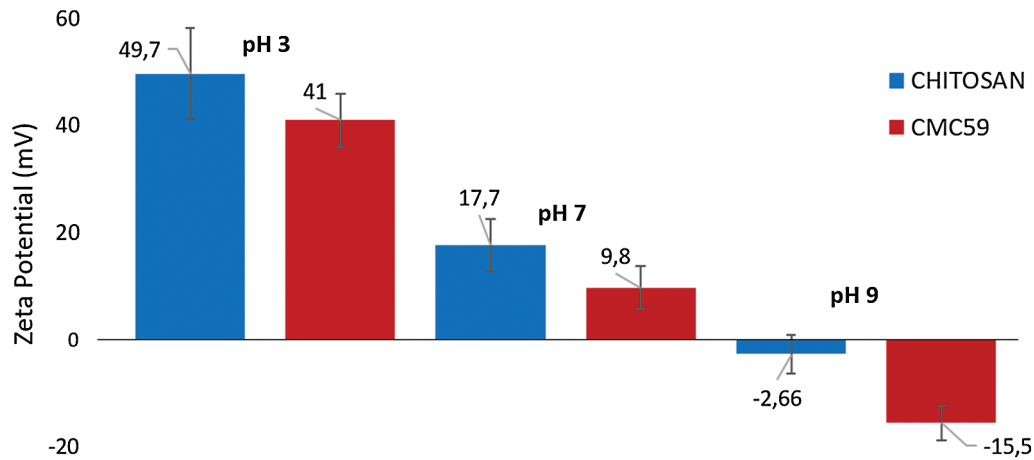


**Figure 7:** Variation of zeta potential as a function of pH for Chitosan and Carboxymethylchitosan (CMC59)

**3.6 Study of the Volume of Sedimentable Solids Formed during the Tests**

The volumes of sedimentable solids (direct measurement of the sludge content generated in the process) obtained for the biocoagulants and aluminum sulphate are shown in Fig. 8. It is easily understood that chitosan and carboxymethylchitosan produce lower volumes of sedimentable solids using much smaller dosages, when compared to  $Al_2(SO_4)_3$ . There was an average reduction of 25% considering the best dosages for removal of color and turbidity of each one, contributing to decrease the amount of solid waste generated at the end of the process. After the treatment, the biocoagulants are discarded with the sludge at the end of the process. However, the residue formed is biodegradable and has lower toxicity than the aluminum sulphate, reducing the environmental impacts. This type of solid waste can be further degraded naturally by microorganisms [6,7].

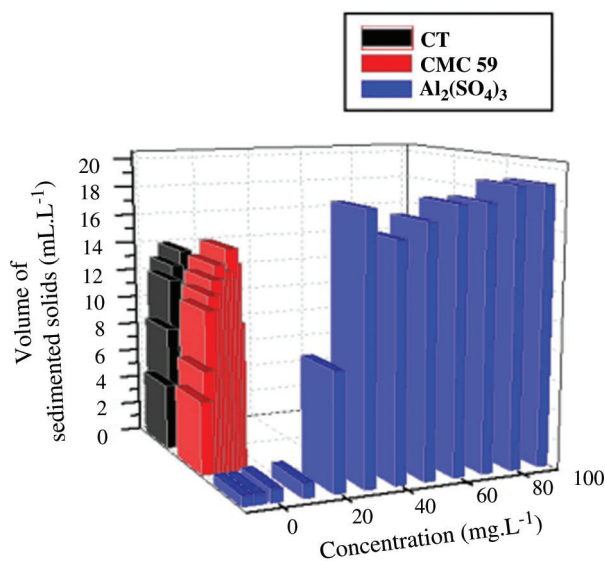


**Figure 8:** Comparison between the formation of sedimentable solids by the use of chitosan, CMC59 and aluminum sulphate as coagulants

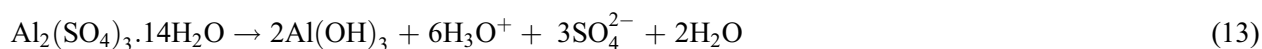
Similar results were found by Hu et al. [1] when comparing sludge production at the end of the treatment process of highly turbid waters (10,000 NTU) using chitosan and  $\text{AlCl}_3$  as coagulants. To obtain equivalent residual turbidity results, concentrations of  $135 \text{ mg l}^{-1}$  of aluminum chloride with  $150 \text{ ml l}^{-1} \text{ H}_2\text{O}$  of sedimentable solids were required, whereas for chitosan only  $5 \text{ mg l}^{-1}$ , with generation of  $30 \text{ ml l}^{-1} \text{ H}_2\text{O}$  of residual sludge. Quantitative data on the production of sedimentable solids by the use of carboxymethylchitosan as biocoagulant is still scarce in the literature and limit possible comparisons with inorganic coagulants.

During sedimentation, the biocoagulants formed rounded flakes, with a few millimeters of diameter, which aggregated in a few seconds (15–20 s) and were quickly deposited in the bottom of the container, forming, over time, large and compact macroflocs. For  $\text{Al}_2(\text{SO}_4)_3$ , it was possible to notice that the flocs formed were bulky, not very dense and with slow sedimentation.

When compared, chitosan and carboxymethylchitosan present peculiar behaviors in the production of sedimentable solids, mainly in concentrations above  $8.0 \text{ mg l}^{-1}$ . Carboxymethylchitosan maintains coagulant efficiency, a direct consequence of its greater solubility in water, but in some concentration ranges it produces a larger volume of sludge. This phenomenon may be associated to the presence of new chemical groups (increase of the atomic volume) and the higher hydrodynamic volume of the polymer in solution (volume of the biopolymer + solvation layer) [32].

### 3.7 Influence of Coagulants on the Electrical Conductivity of the Medium

All coagulants showed a positive relation between ideal concentration and increase in the final electrical conductivity of the treated water, with variations of 340.34% for  $\text{Al}_2(\text{SO}_4)_3$  ( $90 \text{ mg l}^{-1}$ ), 17.95% for chitosan ( $4.0 \text{ mg l}^{-1}$ ) and 69.48% for carboxymethylchitosan ( $7.0 \text{ mg l}^{-1}$ ). As expected, the increase in  $\text{Al}_2(\text{SO}_4)_3$  concentrations promoted an increase in the electrical conductivity of the medium, due to the dissociation and hydrolysis reactions of the salt, briefly summarized in Eq. (1). This trend was also observed by Magaji et al. [33] when conducting comparative studies between aluminum sulphate and biocoagulants in the treatment of river and residual waters.



A very important species produced in the process is the  $\text{H}_3\text{O}^+$  cation, responsible for both the electrical conductivity increase and the significant pH reduction observed during the coagulation tests.

For chitosan, the maximum variation observed was 70.78% ( $12 \text{ mg l}^{-1}$ ), mainly due to the addition of HCl present initially in the coagulant solution. The oscillation in the electrical conductivity values observed for carboxymethylchitosan (230.84% for  $12 \text{ mg l}^{-1}$  dosages) is associated with the exchange of hydroxylic hydrogens (strongly bound to the aminopolysaccharide structure) by the carboxymethyl groups (acids), capable of ionization in the medium, which generate more species that transport negative charges.

## 4 Conclusions

The results of the present study showed the advantages of the application of carboxymethylchitosan to the treatment of highly turbid synthetic waters, showing that the insertion of carboxymethyl groups can be an important tool to overcome the environmental application limitations of chitosan, involving solubility restricted to acidic media. The production of a derivative soluble in acidic, basic and neutral media may allow the use of carboxymethylchitosan for the most varied types of water and effluent treatment. It was observed the maintenance of the coagulation efficiency in a wide pH range, with results of removal of color and turbidity over 99% using lower dosages when compared to aluminum sulphate and other proposed biocoagulants. Minimum residual turbidity and apparent color were obtained without water filtration; by using this process, it is theoretically possible to further decrease the final values of these

parameters, adapting them to what is recommended by the standards of adequacy for bathing and potability established in different nations.

**Acknowledgement:** The authors are grateful to the State University of Ceará and to the Federal Institute of Education, Science and Technology of Ceará—*campus* of Crateús for the concession of equipment and physical structure necessary for the development of the work. The authors would also like to thank the NMR Network of UFRGS by the analysis performed, and Dr. José R. Gregório for the accessories materials and invaluable help in the preparation of the samples.

**Funding Statement:** The authors would like to thank CNPq for financial support [Project Number 442965/2014-1].

**Conflicts of Interest:** The authors declare that they have no conflicts of interest.

## References

1. Hu, C. Y., Lo, S. L., Chang, C. L., Chen, F. L., Wu, Y. D. et al. (2013). Treatment of highly turbid water using chitosan and aluminum salts. *Separation and Purification Technology*, 104, 322–326. DOI 10.1016/j.seppur.2012.11.016.
2. Altaher, H. (2012). The use of chitosan as a coagulant in the pre-treatment of turbid sea water. *Journal of Hazardous Materials*, 233–234, 97–102. DOI 10.1016/j.jhazmat.2012.06.061.
3. Ghernaout, D., Ghernaout, B., Naceur, M. W. (2011). Embodying the chemical water treatment in the green chemistry—a review. *Desalination*, 271(1–3), 1–10. DOI 10.1016/j.desal.2011.01.032.
4. Polizzi, S., Pira, E., Ferrara, M., Bugiani, M., Papaleo, A. et al. (2002). Neurotoxic effects of aluminium among foundry workers and Alzheimer’s disease. *NeuroToxicology*, 23(6), 761–774. DOI 10.1016/S0161-813X(02)00097-9.
5. Banks, W. A., Niehoff, M. L., Drago, D., Zatta, P. (2006). Aluminum complexing enhances amyloid  $\beta$  protein penetration of blood-brain barrier. *Brain Research*, 1116(1), 215–221. DOI 10.1016/j.brainres.2006.07.112.
6. Renault, F., Sancey, B., Badot, P. M., Crini, G. (2009). Chitosan for coagulation/flocculation processes—an eco-friendly approach. *European Polymer Journal*, 45(5), 1337–1348. DOI 10.1016/j.eurpolymj.2008.12.027.
7. Yang, R., Li, H., Huang, M., Yang, H., Li, A. (2016). A review on chitosan-based flocculants and their applications in water treatment. *Water Research*, 95, 59–89. DOI 10.1016/j.watres.2016.02.068.
8. Lima, R. N., Abreu, F. O. M. S. (2018). Natural products used as coagulants and flocculants for public water supply: a review of benefits and potentialities. *Virtual Journal of Chemistry*, 10(3), 709–735. DOI 10.21577/1984-6835.20180052.
9. Bukzem, A. L., Signini, R., dos Santos, D. M., Lião, L. M., Ascheri, D. P. R. (2016). Optimization of carboxymethyl chitosan synthesis using response surface methodology and desirability function. *International Journal of Biological Macromolecules*, 85, 615–624. DOI 10.1016/j.ijbiomac.2016.01.017.
10. Borsagli, F. G. L. M., Mansur, A. A. P., Chagas, P., Oliveira, L. C. A., Mansur, H. S. (2015). O-carboxymethyl functionalization of chitosan: complexation and adsorption of Cd (II) and Cr (VI) as heavy metal pollutant ions. *Reactive and Functional Polymers*, 97, 37–47. DOI 10.1016/j.reactfunctpolym.2015.10.005.
11. Abreu, F. O. M. S., Bianchini, C., Kistb, T. B., Forte, M. M. C. (2009). Preparation and properties of core-shell alginate-carboxymethylchitosan hydrogels. *Polymer International*, 58(11), 1267–1274. DOI 10.1002/pi.2657.
12. Ge, H. C., Luo, D. K. (2005). Preparation of carboxymethyl chitosan in aqueous solution under microwave irradiation. *Carbohydrate Research*, 340(7), 1351–1356. DOI 10.1016/j.carres.2005.02.025.
13. Brugnerotto, J., Lizardi, J., Goycoolea, F. M., Argüelles-Monal, W., Desbrières, J. et al. (2001). An infrared investigation in relation with chitin and chitosan characterization. *Polymer (Guildford)*, 42(8), 3569–3580. DOI 10.1016/S0032-3861(00)00713-8.
14. Gottlieb, H. E., Kotlyar, V., Nudelman, A. (1997). NMR chemical shifts of common laboratory solvents as trace impurities. *Journal of Organic Chemistry*, 62(21), 7512–7515. DOI 10.1021/jo971176v.

15. Chen, X. G., Park, H. J. (2003). Chemical characteristics of O-carboxymethyl chitosans related to the preparation conditions. *Carbohydrate Polymers*, 53(4), 355–359. DOI 10.1016/S0144-8617(03)00051-1.
16. Nordtveit, H. R. J., Vårum, K. M., Grasdalen, H., Tokura, S., Smidsrød, O. (1997). Chemical composition of O-(carboxymethyl)-chitins in relation to lysozyme degradation rates. *Carbohydrate Polymers*, 34(3), 131–139. DOI 10.1016/S0144-8617(97)00113-6.
17. Clesceri, L., Greenberg, A., Eaton, A. (1999). *Standard methods for the examination of water and wastewater*. 20th edition. Washington DC, USA: American Public Health Association.
18. Kusuma, H. S., Al-sa'bani, A. F., Darmokoesoemo, H. (2015). N,O-Carboxymethyl chitosan: an innovation in new natural preservative from shrimp shell waste with a nutritional value and health orientation. *Procedia Food Science*, 3, 35–51. DOI 10.1016/j.profoo.2015.01.004.
19. Abreu, F. R., Campana-Filho, S. P. (2005). Preparation and characterization of carboxymethylchitosan. *Polímeros*, 15(2), 79–83. DOI 10.1590/s0104-14282005000200004.
20. Lee, C. S., Robinson, J., Chong, M. F. (2014). A review on application of flocculants in wastewater treatment. *Process Safety and Environmental Protection*, 92(6), 489–508. DOI 10.1016/j.psep.2014.04.010.
21. Sánchez-Martín, J., González-Velasco, M., Beltrán-Heredia, J. (2010). Surface water treatment with tannin-based coagulants from Quebracho (*Schinopsis balansae*). *Chemical Engineering Journal*, 165(3), 851–858. DOI 10.1016/j.cej.2010.10.030.
22. Yang, Z., Shang, Y., Lu, Y., Chen, Y., Huang, X. et al. (2011). Flocculation properties of biodegradable amphoteric chitosan-based flocculants. *Chemical Engineering Journal*, 172(1), 287–295. DOI 10.1016/j.cej.2011.05.106.
23. Zhao, D., Xu, J., Wang, L., Du, J., Dong, K. et al. (2012). Study of two chitosan derivatives phosphorylated at hydroxyl or amino groups for application as flocculants. *Journal of Applied Polymer Science*, 125(S2), E299–E305. DOI 10.1002/app.36834.
24. Oladoja, N. A., Saliu, T. D., Ololade, I. A., Anthony, E. T., Bello, G. A. (2017). A new indigenous green option for turbidity removal from aqueous system. *Separation and Purification Technology*, 186, 166–174. DOI 10.1016/j.seppur.2017.05.054.
25. Abidin, Z. Z., Shamsudin, N. S. M., Madehi, N., Sobri, S. (2013). Optimisation of a method to extract the active coagulant agent from *Jatropha curcas* seeds for use in turbidity removal. *Industrial Crops and Products*, 41, 319–323. DOI 10.1016/j.indcrop.2012.05.003.
26. Sillanpää, M., Ncibi, M. C., Matilainen, A., Vepsäläinen, M. (2018). Removal of natural organic matter in drinking water treatment by coagulation: a comprehensive review. *Chemosphere*, 190, 54–71. DOI 10.1016/j.chemosphere.2017.09.113.
27. Khodapanah, N., Ahamad, I. S., Idris, A. (2013). Potential of using bio-coagulants indigenous to Malaysia for surface water clarification. *Research Journal of Chemical and Environment*, 17, 70–75.
28. Peralta-Zamora, P., Esposito, E., Reyes, J., Durán, N. (1997). Remediação de efluentes derivados da indústria de papel e celulose: tratamento biológico e fotocatalítico. *Química Nova*, 20(2), 186–190. DOI 10.1590/S0100-40421997000200010.
29. Edogbanya, O., Abolude, D., Adelanwa, M., Ocholi, O. (2016). The efficacy of the seeds of *Adansonia digitata* L. as a biocoagulant and disinfectant in water purification. *Journal of Earth, Environment and Health Sciences*, 2(3), 122–128. DOI 10.4103/2423-7752.199289.
30. Liu, X. F., Guan, Y. L., Yang, D. Z., Li, Z., Yao, K. D. (2001). Antibacterial action of chitosan and carboxymethylated chitosan. *Journal of Applied Polymer Science*, 79, 1324–1335.
31. Wang, L. C., Chen, X. G., Liu, C. S., Li, P. W., Zhou, Y. M. (2008). Dissociation behaviors of carboxyl and amine groups on carboxymethyl-chitosan in aqueous system. *Journal of Polymer Science Part B: Polymer Physics*, 46(14), 1419–1429. DOI 10.1002/polb.21475.
32. Mourya, V. K., Inamdar, N. N., Tiwari, A. (2010). Carboxymethyl chitosan and its applications. *Advanced Materials Letters*, 1(1), 11–33. DOI 10.5185/amlett.2010.3108.
33. Magaji, U. F., Sahabi, D. M., Abubakar, M. K., Muhammad, A. B. (2015). Biocoagulation activity of moringa oleifera seeds for water treatment. *The International Journal of Engineering and Science*, 4, 19–26.